(Received 4 May 2024, Accepted 3 July 2024, Scheduled 5 July 2024)

Study on AC Loss Suppression in Rectangular Winding Motors for Electric Vehicles

Shengyang Xu and Quanfeng Li*

School of Electrical Engineering, Shanghai DianJi University, China

ABSTRACT: Currently, excessive AC loss in the rectangular winding motor used for electric vehicles poses a significant challenge, necessitating effective measures to suppress the losses. This paper focuses on the Prius IV motor, employing a finite element two-dimensional model established using JMAG software. The influence of conductor material and the number of rectangular winding layers on motor AC loss under various operating conditions is thoroughly analyzed. Maintaining a constant number of rectangular winding layers, aluminum (Al) conductors replace copper (Cu) conductors in 2-layer, 4-layer, 6-layer, and 8-layer configurations, respectively. AC losses are compared among motors with 4-layer, 6-layer, 8-layer, and 10-layer Cu rectangular windings, all having identical slot dimensions. Subsequently, the 10-layer Al conductor scheme is chosen to optimize motor design. The results demonstrate an average reduction in AC loss up to 59.24% after motor optimization, further reducing motor manufacturing costs.

1. INTRODUCTION

Electric vehicles offer several advantages, including energy savings, environmental protection, cost-effectiveness, high efficiency, and low noise [1]. These benefits present significant development opportunities, especially in the context of the current energy shortage. As the core component of electric vehicles, electric drive system plays a crucial role in determining the vehicle's power, economy, safety, comfort, and longevity. Within the electric drive system, the motor stands out as the central element, with its performance largely dictating the overall performance of the vehicle. The characteristics of motors for electric vehicles are extensively studied by scholars [2, 3].

In the 14th Five-Year Plan [4], China proposed to deeply implement the strategy of becoming a manufacturing powerhouse, focusing on breakthroughs in key technologies for high-efficiency drive motors for electric vehicles. This plan aims to promote the high-quality development of the automobile manufacturing industry. In recent years, rectangular winding motors have gained widespread use in electric vehicle drive motors due to their significant advantages, such as reduced material usage and improved thermal conductivity [5]. Currently, the maximum speed of Tesla's 2023 Model S Plaid motor reaches 20,000 rpm. China's Huawei has developed the new-generation Drive ONE 800V intelligent electric drive platform, which can reach a maximum speed of 22,000 rpm. Additionally, Xiaomi's self-researched and mass-produced Hyper Engine V8s motor achieves speeds as high as 27,200 rpm. The increasing peak speeds contribute to the drive motor's advancement towards lightweight design.

However, due to the skin effect and proximity effect, the issue of AC losses in rectangular windings becomes increasingly severe when the motor operates at high speeds. The increase in AC loss results in a higher temperature rise of the motor, increasing the risk of demagnetization of permanent magnets at high temperatures and thus threatening the operational safety of the motor. Consequently, extensive research has been conducted to address the problem of AC losses in rectangular winding motors.

Mellor et al. proposed an analytical approach to accurately model winding AC loss and its temperature dependence [6]. The influence of saturation in AC loss was considered by Moros et al. [7]. AC losses were calculated from the perspective of energy flow by Wang et al. using Poincarétin vectors [8, 9]. The end loss of rectangular winding was analyzed by Aoyama and Deng using 3D finite element simulation [10]. The results showed that the loss in the slot winding is greater than the end winding.

In [11], a 72-slot, 12-pole permanent magnet synchronous motor with a peak speed of 15,000 r/min and a peak torque of 190 N · m was examined. A design of rectangular winding with unequal heights was proposed, resulting in a more uniform distribution of losses in the conductor, significantly reducing AC losses, improving motor efficiency, and increasing peak continuous output power. Preci et al. compared the AC losses of random windings, hairpin windings, and segmented hairpin windings under three different operating conditions [12]. The results showed that segmented hairpin windings can reduce AC losses by 10–20%.

The difference between AC losses in same-phase and different-phase slots of rectangular winding was investigated by Wang et al. [13]. It was found that a reasonable allocation of conductors belonging to different phases in the same slot can effectively reduce AC losses. Liang et al., through analytical calculations and three-dimensional finite element analysis, demonstrated that AC losses of the motor were reduced by

* Corresponding author: Quanfeng Li (lqf108359@163.com).

44.55% by using formed transposition windings instead of hairpin windings [14].

In summary, a series of research studies has been conducted on the AC loss of rectangular winding motors, focusing on various measures to suppress AC loss. In this paper, based on previous research, a Prius IV motor is used as the research object. A two-dimensional model of the motor is established using JMAG finite element analysis software. The influence of conductor material and rectangular winding layer on the AC loss of the motor is studied. To minimize the AC loss, a scheme using 10-layer aluminum rectangular windings is employed.

2. CALCULATION OF LOSSES IN RECTANGULAR WINDING

The DC loss, which occurs due to the current flowing through the winding resistance, can be calculated using the following formula:

$$P_{\mathrm{DC}} = mI_{\mathrm{rms}}^2 R_{\mathrm{DC}} \tag{1}$$

In (1), m represents the number of phases of the motor. Typically, the motor under consideration is a three-phase motor, so $m = 3$. I_{rms} denotes the root mean square (RMS) value of the phase current. R_{DC} is the resistance of a single-phase winding.

The AC loss, which accounts for losses due to alternating current flowing through the winding and factors such as skin effect and proximity effect, can be calculated using the following formula:

$$P_{\mathrm{AC}} = mK_R I_{\mathrm{rms}}^2 R_{\mathrm{DC}} \tag{2}$$

In (2), K_R is the AC resistance factor introduced due to the skin effect.

AC resistance factor can be calculated from (3) [15]:

$$K_R = 1 + \frac{z_t^2 - 0.2}{9} h_{\mathrm{c0}}^4 \left(\frac{\pi f \mu_0 \sigma_{\mathrm{c}} b_{\mathrm{c}}}{b} \right) \tag{3}$$

In (3), z_t is the number of conductors in the stator slot; h_{c0} is the height of each conductor in the slot; b_{c} is the width of each conductor in the slot; b is the stator slot width; f is the frequency of alternating current; μ_0 is the vacuum permeability; σ_{c} is the conductivity of conductor material.

From (3), it is evident that the AC resistance factor K_R is intricately linked to various factors such as conductor dimensions, material properties, slot geometry, and current frequency. Additionally, it can be influenced by temperature variations, slot leakage flux, and other practical factors, making precise analytical determination challenging.

The total winding loss can be obtained by adding (1) and (2), as shown in (4).

$$P_{\mathrm{Total}} = P_{\mathrm{AC}} + P_{\mathrm{DC}} \tag{4}$$

3. FINITE ELEMENT SIMULATION OF MOTOR

In this section, the Prius IV motor is analyzed as the research object, with the main parameters presented in Table 1. To save computational time, a 1/8 model is used for the simulation, as shown in Fig. 1.

Since the quality of mesh dissections directly determines the accuracy of finite element calculations, fine dissections of the windings are required to accurately calculate the winding losses. Considering the influence of the skin effect, the skin depth mesh is refined using JMAG software. A schematic diagram of the conductor mesh dissection is shown in Fig. 2.

Finite element simulation calculations are performed on the motor to obtain the winding current density cloud and loss density cloud as shown in Fig. 3 and Fig. 4.

TABLE 1. Prius IV main parameters.

Parameter	Value
Slot/pole	48/8
Stator outer diameter/mm	215
Stator inner diameter/mm	141.8
Airgap length/mm	0.7
Rotor inner diameter /mm	47.3
Slot depth/mm	18.42
Slot width/mm	4.15
Conductor width/mm	3.4
Conductor height/mm	2.05
Number of conductors per slot	8

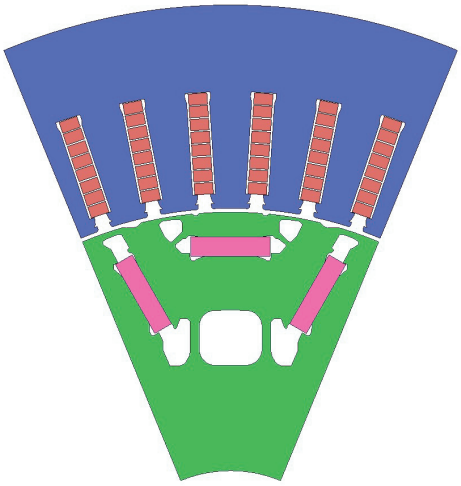

FIGURE 1. Prius IV 1/8 model.

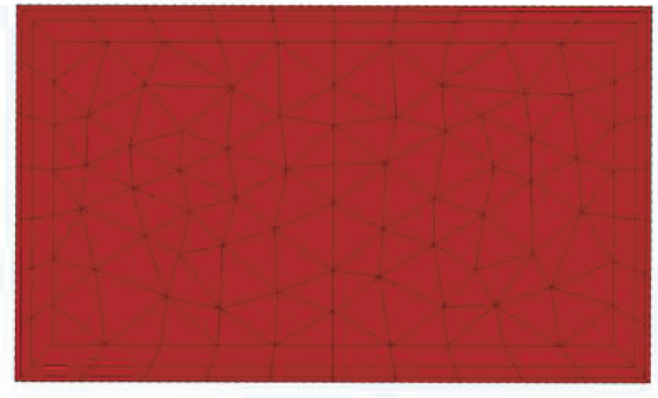

FIGURE 2. Conductor mesh dissection.

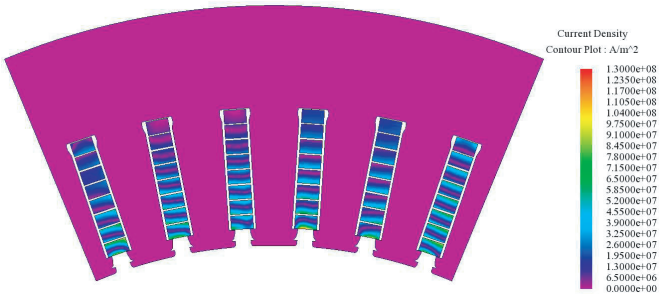

FIGURE 3. Winding current density cloud.

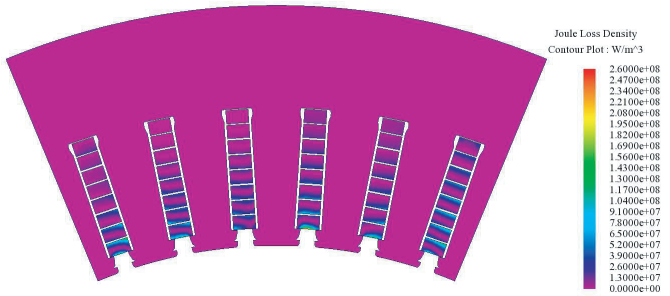

FIGURE 4. Winding current density cloud.

Figures 3 and 4 illustrate that the current density and loss density in the winding gradually decrease from the slot opening conductor to the bottom conductor. This phenomenon is primarily due to the significantly larger leakage flux at the slot opening than the bottom of the slot. The leakage flux induces eddy currents in the conductor, resulting in additional losses. Therefore, the width of the slot opening has a certain impact on the winding loss.

Table 2 and Fig. 5 show the distribution of DC losses, AC losses, and total losses at different speeds, obtained by varying the current frequency of the motor under a 100 A current excitation.

TABLE 2. Winding loss distribution at different speeds.

Speed/rpm	Total loss/W	DC loss/W	AC loss/W
1000	574.59	562.81	11.78
3000	671.42	562.81	108.62
5000	855.07	562.81	292.26
7000	1118.04	562.81	555.23
10000	1648.31	562.81	1085.50
12000	2085.23	562.81	1522.42
15000	2855.14	562.81	2292.33

From Table 2 and Fig. 5, it is evident that under low-speed (1000 rpm–3000 rpm) and medium-speed (5000 rpm–7000 rpm) conditions, the DC loss is greater than the AC loss. However, at high speeds (10,000 rpm and above), the AC loss gradually exceeds the DC loss. At 15,000 rpm, the AC loss is approximately three times the DC loss, becoming the primary source of winding loss.

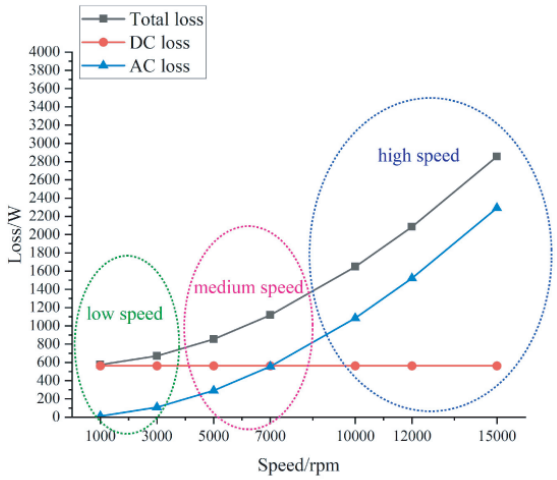

FIGURE 5. Winding loss at different speeds.

4. ANALYSIS OF AC LOSS SUPPRESSION IN RECTANGULAR WINDING MOTORS

From the above analysis, it is clear that the AC loss generated by the rectangular winding motor operating under high-speed and high-frequency conditions is significantly larger than the DC loss, seriously affecting the motor's efficiency. Therefore, using the Prius IV motor as a basis, this section focuses on optimizing the design by adjusting the conductor material and the number of winding layers, thereby reducing the motor's AC loss.

4.1. Optimization Design Based on Conductor Material

As shown in (3), the AC resistance factor K_R increases with rising current frequency. Consequently, the AC loss can be suppressed by increasing the resistance of the conductor material, which is achieved by reducing the material's conductivity σ_c.

Based on the consideration of conductivity and cost of different materials, an Al conductor is selected to replace the Cu conductor in the study.

The conductivity of Cu conductor at room temperature is $\sigma_{Cu} = 59.77 \times 10^6$ S/m, and the conductivity of Al conductor is $\sigma_{Al} = 37.66 \times 10^6$ S/m. As depicted in Fig. 6, the schemes are outlined as follows:

Scheme 1: Utilizes 8 Cu conductors;

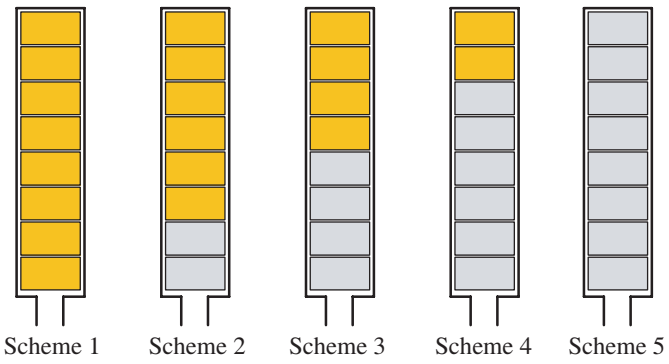

FIGURE 6. Different conductor material schemes.

Scheme 2: Replaces 2 Cu conductors near the slot opening with Al;

Scheme 3: Comprises half Cu conductors and half Al;

Scheme 4: Replaces 2 Cu conductors near the bottom of the slot with Al;

Scheme 5: Utilizes 8 Al conductors.

Similarly, under the condition of a given 100 A current excitation, the loss distribution for each scheme at different speeds is simulated using finite element analysis. The results are presented in Tables 3 to 6, while the loss distribution for Scheme 1 is provided in Table 2.

TABLE 3. Scheme 2 winding loss distribution.

Speed/rpm	Total loss/W	DC loss/W	AC loss/W
1000	654.114	645.03	9.084
3000	729.64	645.03	84.61
5000	874.504	645.03	229.474
7000	1083.65	645.03	438.62
10000	1508.8	645.03	863.77
12000	1861.37	645.03	1216.34
15000	2486.31	645.03	1841.28

TABLE 4. Scheme 3 winding loss distribution.

Speed/rpm	Total loss/W	DC loss/W	AC loss/W
1000	735.407	727.401	8.006
3000	802.172	727.401	74.771
5000	930.447	727.401	203.046
7000	1115.89	727.401	388.489
10000	1493.58	727.401	766.179
12000	1807.38	727.401	1079.979
15000	2364.83	727.401	1637.429

TABLE 5. Scheme 4 winding loss distribution.

Speed/rpm	Total loss/W	DC loss/W	AC loss/W
1000	817.399	809.824	7.575
3000	880.694	809.824	70.87
5000	1002.48	809.824	192.656
7000	1178.81	809.824	368.986
10000	1538.74	809.824	728.916
12000	1838.89	809.824	1029.066
15000	2371.71	809.824	1561.886

Figures 7, 8, and 9 illustrate the distributions of DC loss, AC loss, and total loss with speed for the different schemes. The data indicates that as the number of layers of Al conductors increases, the DC loss of the motor increases while the AC loss decreases. At low speeds, increasing the number of Al conductor layers results in a higher total loss of the motor. However, when the speed reaches 10,000 rpm and above, the AC loss is effectively suppressed, leading to a reduction in the total loss. Thus, increasing the number of layers of Al conductors can effectively suppress AC loss and reduce total loss at high speeds, despite the increase in DC loss at low speeds.

TABLE 6. Scheme 5 winding loss distribution.

Speed/rpm	Total loss/W	DC loss/W	AC loss/W
1000	899.7	892.264	7.436
3000	961.923	892.264	69.659
5000	1081.86	892.264	189.596
7000	1255.87	892.264	363.606
10000	1611.88	892.264	719.616
12000	1908.86	892.264	1016.596
15000	2438.31	892.264	1546.046

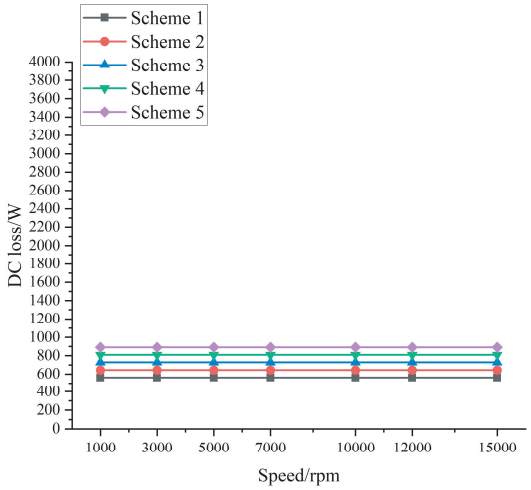

FIGURE 7. DC loss distribution under different schemes.

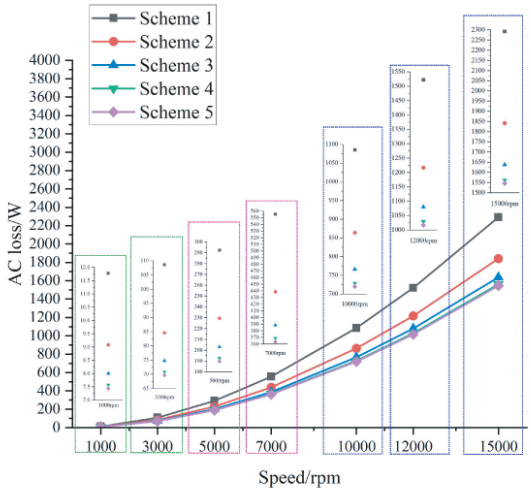

FIGURE 8. AC loss distribution under different schemes.

4.2. Optimization Design Based on Different Conductor Layers

In (3), the height of each conductor in the slot h_{c0} affects the variation of the AC resistance factor K_R, so the AC loss can be suppressed by changing the height of each conductor in the slot.

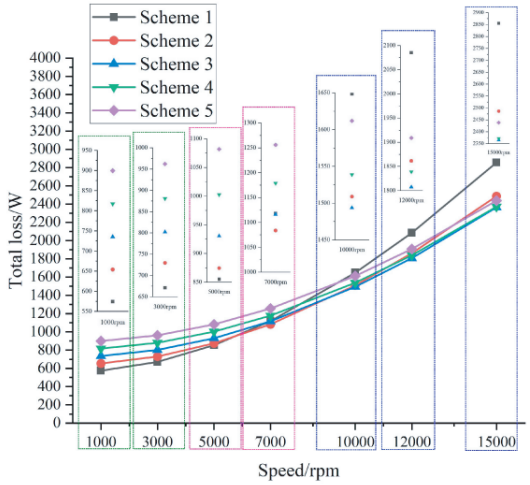

FIGURE 9. Total loss distribution under different schemes.

As shown in Fig. 10, while maintaining a constant conductor width, the heights of the conductors are modified to 4.01 mm, 2.80 mm, 2.05 mm, and 1.60 mm, corresponding to 4, 6, 8, and 10 layers, respectively.

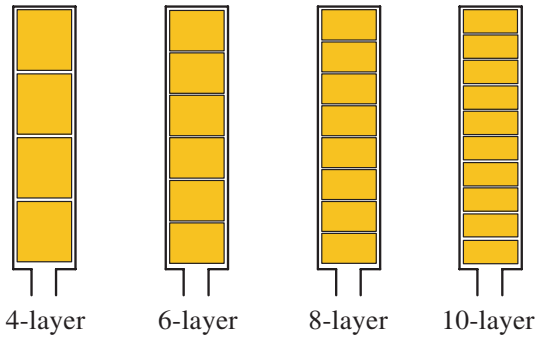

FIGURE 10. Distribution of Cu conductor layers.

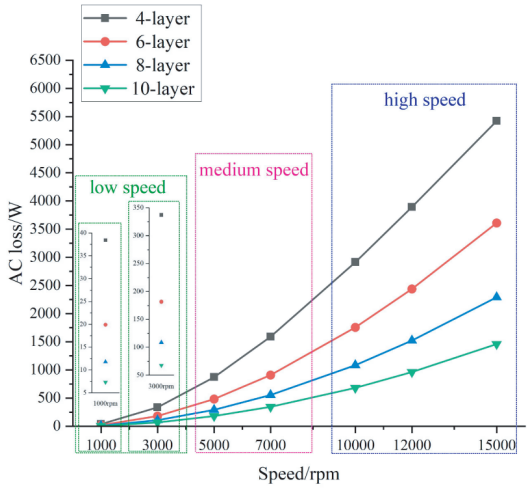

FIGURE 11. AC loss distribution under different layers of Cu rectangular winding.

For 4-layer, 6-layer, 8-layer, and 10-layer schemes, the current through each conductor is set to 25 A, 16.67 A, 12.5 A, and 10 A, respectively, to ensure uniformity in the number of slot ampere-turns. Based on this premise, the loss distribution under different conductor layers is calculated by finite element simulation, as shown in Tables 7, 8, and 9. The loss distribution of 8-layer rectangular winding is consistent with Table 2.

TABLE 7. Winding loss distribution of 4-layer.

Speed/rpm	Total loss/W	DC loss/W	AC loss/W
1000	602.91	564.49	38.42
3000	901.58	564.49	337.09
5000	1436.33	564.49	871.84
7000	2155.90	564.49	1591.41
10000	3477.80	564.49	2913.31
12000	4457.74	564.49	3893.25
15000	5987.10	564.49	5422.61

TABLE 8. Winding loss distribution of 6-layer.

Speed/rpm	Total loss/W	DC loss/W	AC loss/W
1000	569.86	549.95	19.90
3000	731.48	549.95	181.53
5000	1033.86	549.95	483.91
7000	1460.68	549.95	910.73
10000	2305.64	549.95	1755.69
12000	2987.95	549.95	2438.00
15000	4161.16	549.95	3611.21

TABLE 9. Winding loss distribution of 10-layer.

Speed/rpm	Total loss/W	DC loss/W	AC loss/W
1000	583.81	576.51	7.31
3000	643.81	576.51	67.30
5000	758.07	576.51	181.56
7000	923.07	576.51	346.56
10000	1259.50	576.51	682.99
12000	1539.47	576.51	962.96
15000	2037.66	576.51	1461.15

As shown in Figs. 11–12, under low-speed conditions, the difference in loss across different conductor layers is minimal. However, as the speed exceeds 10,000 rpm, the suppression of AC loss becomes more pronounced with an increasing number of winding layers. At a speed of 15,000 rpm, the AC loss for a 10-layer Cu rectangular winding is 73.05%, 59.54%, and 36.26% lower than that of 4-layer, 6-layer, and 8-layer Cu rectangular windings, respectively.

Therefore, it is feasible to suppress AC loss by reducing the conductor height, that is, increasing the number of layers of rectangular winding.

5. COMPARATIVE ANALYSIS OF MOTOR OPTIMIZATION SCHEMES

From the above analysis, it is evident that using Al conductors instead of Cu conductors, along with increasing the num-

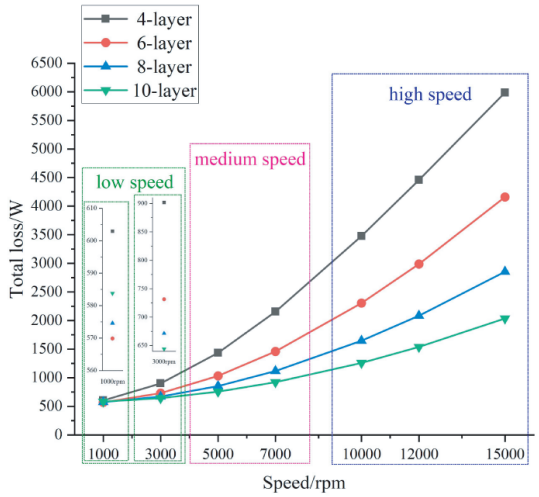

FIGURE 12. Total loss distribution under different layers of Cu rectangular winding.

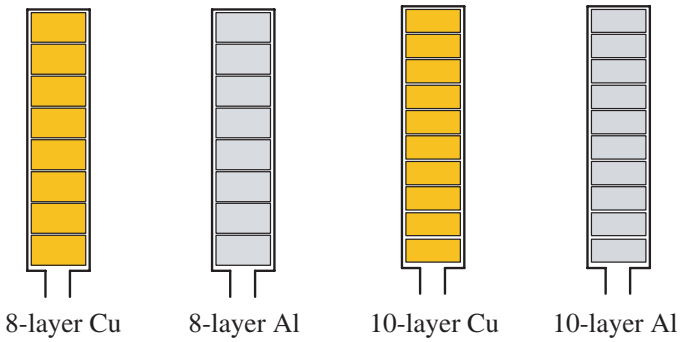

FIGURE 13. Comparison of 4 schemes.

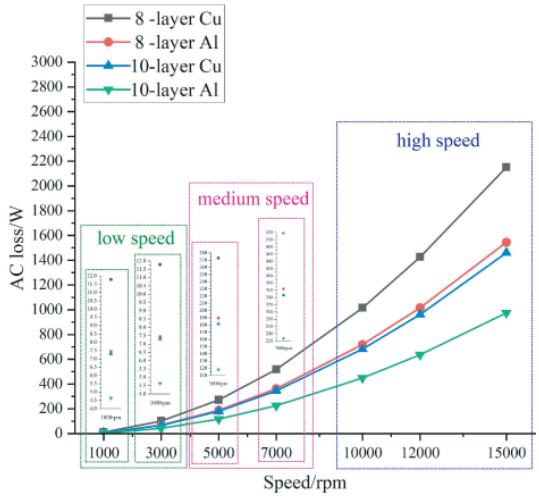

FIGURE 14. AC loss distribution of 4 schemes.

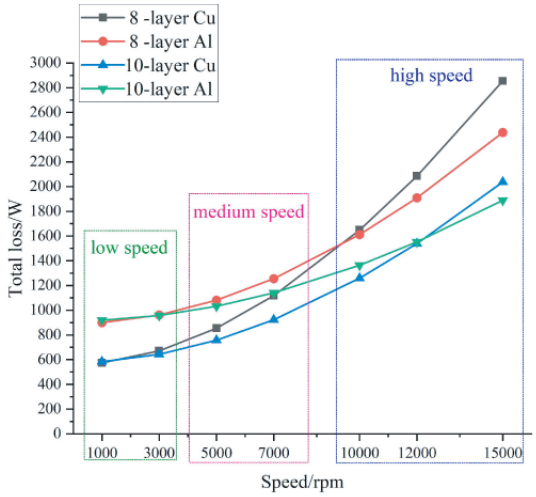

FIGURE 15. Total loss distribution of 4 schemes.

TABLE 10. AC loss distribution of 4 schemes.

Speed/rpm	8-layer Cu/W	8-layer Al/W	10-layer Cu/W	10-layer Al/W
1000	11.78	7.436	7.307	4.64
3000	101.76	69.659	67.302	43.36
5000	272.86	189.596	181.564	117.97
7000	518.51	363.606	346.563	226.55
10000	1015.34	719.616	682.993	450.13
12000	1425.81	1016.596	962.963	637.94
15000	2150.89	1546.046	1461.153	975.11

ber of layers of rectangular windings, can effectively suppress AC losses. Therefore, this section compares and analyzes the losses of four schemes: 8-layer Cu rectangular winding, 8-layer Al rectangular winding, 10-layer Cu rectangular winding, and 10-layer Al rectangular winding, as shown in Fig. 13.

Finite element simulations of the motor were carried out at different speeds, ensuring that the number of slot ampere turns remained constant for the four schemes. The AC loss and total loss distributions for each scheme are presented in Table 10 and Table 11.

TABLE 11. Total loss distribution of 4 schemes.

Speed/rpm	8-layer Cu/W	8-layer Al/W	10-layer Cu/W	10-layer Al/W
1000	574.59	899.7	583.81	918.976
3000	671.42	961.923	643.81	957.7
5000	855.07	1081.86	758.07	1032.31
7000	1118.04	1255.87	923.07	1140.89
10000	1648.31	1611.88	1259.50	1364.47
12000	2085.23	1908.86	1539.47	1552.28
15000	2855.14	2438.31	2037.66	1889.45

As shown in Fig. 14, with the increase in speed, the AC losses of the 8-layer Cu rectangular winding, 8-layer Al rectangular winding, 10-layer Cu rectangular winding, and 10-layer Al rectangular winding decrease sequentially. Compared to the 8-layer Cu rectangular winding scheme, the average AC loss of the 10-layer Al rectangular winding scheme at different speeds is reduced by 56.67%.

As depicted in Fig. 15, at low speeds, the total loss of the Cu rectangular winding is about 63% of that of the Al rectangular winding. At medium speeds, the total loss of the Cu rectangular winding increases more than that of the Al rectangular winding. At 7,000 rpm, the total loss of the 8-layer Cu rectangular winding is only 22.85 W less than that of the 10-layer Al rectangular winding. Under high-speed conditions, the total loss of the 8-layer Cu rectangular winding exceeds that of the other schemes. At 15,000 rpm, the total loss of the 10-layer Al rectangular winding is about 66% of that of the 8-layer Cu rectangular winding.

Therefore, a 10-layer Al rectangular winding can be used instead of an 8-layer Cu rectangular winding to effectively suppress AC loss and total loss at high speeds.

6. CONCLUSION

In this paper, a Prius IV motor serves as the research subject, and an in-depth study is conducted on the influence of conductor material and the number of layers in rectangular winding on the AC losses of the motor. The research findings are summarized as follows:

At high speeds, increasing the number of layers of Al rectangular windings can significantly reduce the AC loss of the motor. When the motor operates at 10,000 rpm, 12,000 rpm, and 15,000 rpm, the AC loss with 8-layers Al rectangular windings is reduced by 33.71%, 33.22%, and 32.56%, respectively, compared to 8-layers Cu rectangular winding. The total loss is reduced by 2.21%, 8.46%, and 14.60%, respectively.

Reducing the conductor height, i.e., increasing the number of layers of rectangular windings, can suppress the AC losses and total losses of the motor. When the motor operates at 15,000 rpm, the AC losses of the 10-layer Cu rectangular windings are reduced by 73.05%, 59.54%, and 36.26% compared to the 4-layer, 6-layer, and 8-layer Cu rectangular windings, respectively. Correspondingly, the total losses are reduced by 65.97%, 51.03%, and 28.63%, respectively.

With the optimized solution of replacing the 8-layer Cu conductor with a 10-layer Al conductor, the AC losses of the motor have been significantly suppressed, achieving an average reduction of 56.67%. Meanwhile, the total loss is reduced accordingly, amounting to 66.18% of the pre-optimization loss.

REFERENCES

[1] Zeng, J., F. Huang, Y. Zhao, and N. Gao, "Technology status and development trend of new energy vehicle," *Automobile Applied Technology*, Vol. 48, No. 14, 189–194, 2023.

[2] Li, Q., S. Liu, and Y. Hu, "Vibration characteristics of permanent magnet motor stator system based on vibro-inertance matrix method," *IEEE Transactions on Energy Conversion*, Vol. 37, No. 3, 1777–1788, Sep. 2022.

[3] Li, Q., S. Liu, X. Li, and Y. Hu, "Vibro-inertance matrix supported OCF characteristics analysis of PMSM under multiple operating conditions for EV," *IEEE Transactions on Industrial Electronics*, Vol. 71, No. 1, 126–137, Jan. 2024.

[4] Central People's Government of the People's Republic of China, "Outline of the 14th five-year plan (2021–2025) for national economic and social development and vision 2035 of the people's republic of china," https://www.gov.cn/xinwen/2021-03/13/content_5592681.htm.

[5] Venturini, G., M. Carbonieri, L. D. Leonardo, and M. Popescu, "Hairpin windings for traction machines: Analysis and comparison," in *2022 International Conference on Electrical Machines (ICEM)*, 1655–1661, Valencia, Spain, 2022.

[6] Mellor, P., R. Wrobel, and N. Simpson, "AC losses in high frequency electrical machine windings formed from large section conductors," in *2014 IEEE Energy Conversion Congress and Exposition (ECCE)*, 5563–5570, Pittsburgh, PA, USA, 2014.

[7] Moros, S., S. Tenner, J. Kempkes, and U. Schäfer, "The influence of saturation on eddy currents in form-wound windings of electrical machines," in *2020 International Conference on Electrical Machines (ICEM)*, Vol. 1, 1601–1607, Gothenburg, Sweden, 2020.

[8] Wang, L., B. Kou, and W. Cai, "Research on resistance enhancement coefficient and thermal dissipation of stator strands in huge synchronous generator," *IEEE Access*, Vol. 8, 40 357–40 366, 2020.

[9] Zhao, J., H. Guo, L. Wang, and M. Han, "Computer modeling of the Eddy current losses of metal fasteners in rotor slots of a large nuclear steam turbine generator based on finite-element method and deep gaussian process regression," *IEEE Transactions on Industrial Electronics*, Vol. 67, No. 7, 5349–5359, Jul. 2020.

[10] Aoyama, M. and J. Deng, "Visualization and quantitative evaluation of eddy current loss in bar-wound type permanent magnet synchronous motor for mild-hybrid vehicles," *CES Transactions on Electrical Machines and Systems*, Vol. 3, No. 3, 269–278, Sep. 2019.

[11] Islam, M. S., I. Husain, A. Ahmed, and A. Sathyan, "Asymmetric bar winding for high-speed traction electric machines," *IEEE Transactions on Transportation Electrification*, Vol. 6, No. 1, 3–15, Mar. 2020.

[12] Preci, E., G. Valente, A. Bardalai, T. Transi, T. Zou, D. Gerada, M. Degano, G. Buticchi, and C. Gerada, "Rectangular and random conductors: AC losses evaluations and manufacturing considerations," in *IECON 2020 The 46th Annual Conference of the IEEE Industrial Electronics Society*, 1076–1081, Singapore, 2020.

[13] Wang, Y., J. Pries, K. Zhou, H. Hofmann, and D. Rizzo, "Computationally efficient AC resistance model for stator winding with rectangular conductors," *IEEE Transactions on Magnetics*, Vol. 56, No. 4, 1–9, Apr. 2020.

[14] Liang, Y., F. Zhao, K. Xu, W. Wang, J. Liu, and P. Yang, "Analysis of copper loss of permanent magnet synchronous motor with formed transposition winding," *IEEE Access*, Vol. 9, 101 105–101 114, 2021.

[15] Zheng, H., Z. Wang, and S. Yang, "Power loss analysis of PMSM for electric vehicle," *Automobile applied technology*, Vol. 49, No. 2, 42–46, 2024.